OMTN, Volume *29*

Supplemental information

Developing antisense oligonucleotides for a *TECPR2* mutation-induced, ultra-rare neurological disorder using patient-derived cellular models

Luis A. Williams, David J. Gerber, Amy Elder, Wei Chou Tseng, Valeriya Baru, Nathaniel Delaney-Busch, Christina Ambrosi, Gauri Mahimkar, Vaibhav Joshi, Himali Shah, Karthiayani Harikrishnan, Hansini Upadhyay, Sakthi H. Rajendran, Aishwarya Dhandapani, Joshua Meier, Steven J. Ryan, Caitlin Lewarch, Lauren Black, Julie Douville, Stefania Cinquino, Helen Legakis, Karsten Nalbach, Christian Behrends, Ai Sato, Lorenzo Galluzzi, Timothy W. Yu, Duncan Brown, Sudhir Agrawal, David Margulies, Alan Kopin, and Graham T. Dempsey

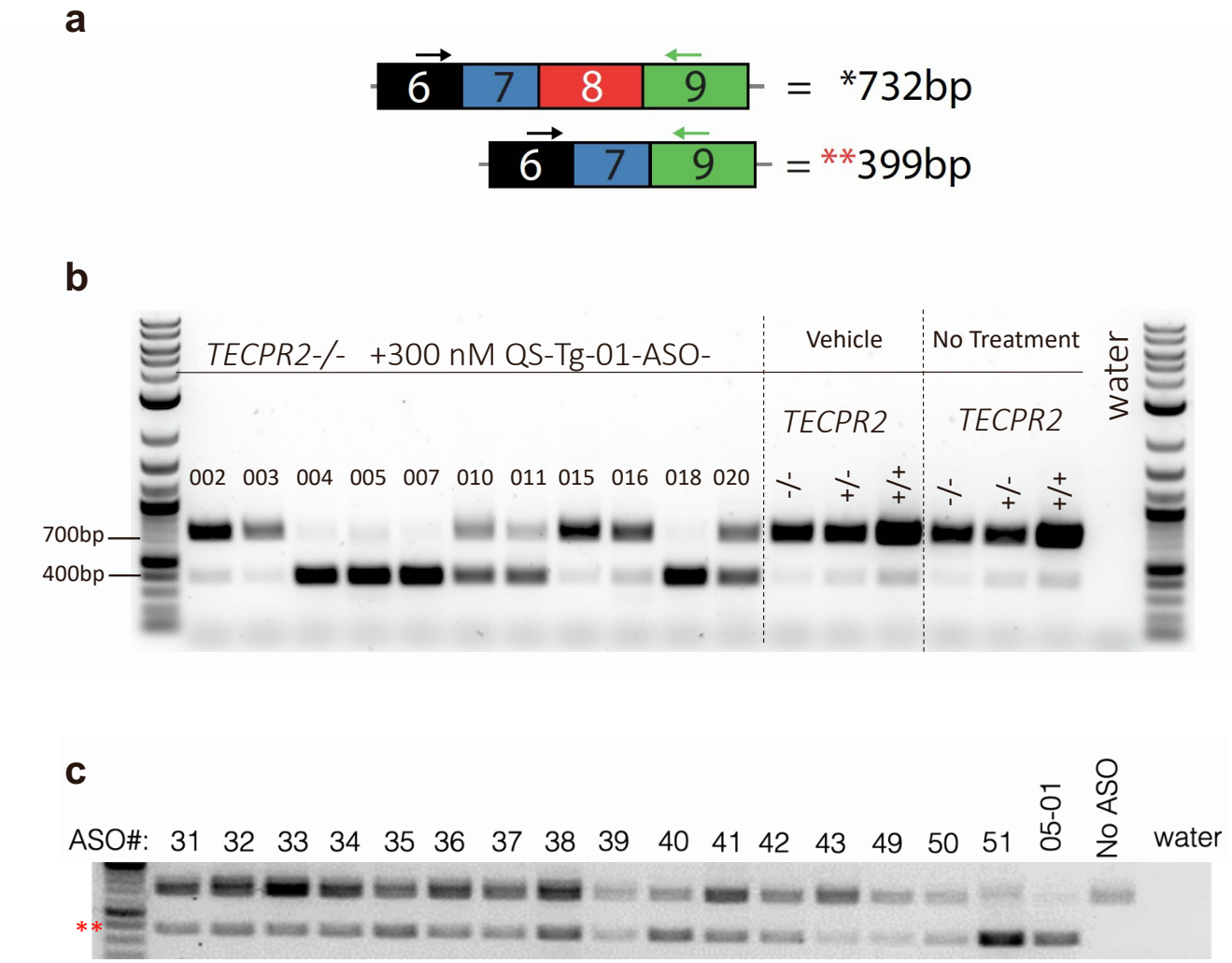

Supplementary Figure 1: Subsequent ASO screening with optimized experimental conditions and additional ASO tiling experiments. **a**, Diagram of RT-PCR assay and PCR amplicons to be obtained when *TECPR2* exon 8 is skipped in human fibroblasts. **b**, Additional ASO screening assay using reduced ASO concentration (300 nM versus 1 μM) and increased incubation time (120 hours versus 72 hours) identified active ASOs targeting the 3' end of *TECPR2* Exon 8 (ASO-018 and ASO-020). cDNA from *TECPR2-/-*, *TECPR2+/-* and *TECPR2+/+* fibroblasts treated with vehicle only (transfection reagent) or exposed to no treatment were used as negative controls. Significant enrichment of lower PCR product (~399bp,**), corresponding to *TECPR2ΔExon8* transcript, can be detected in samples from fibroblasts treated with ASO-004, ASO-005, ASO-007, ASO-010, ASO-011, ASO-018 and ASO-020. **c**, PCR results from additional ASO tiling experiments (1 μM ASO treatment for 72 hours) in TECPR2-/- patient fibroblasts covering the *TECPR2* region homologous to Cynomolgus *TECPR2* within the initially identified positive region for ASO-mediated Exon 8 skipping.

ASO ID	Length (mer)	ASO Sequence (5' to 3')
ASO-020	25	GCTACAGAGGGTACCTGTCTTCTTC
ASO-021	25	AGACATCTCCAGACCATCTCTCACT
ASO-022	25	CCAGACATCTCCAGACCATCTCTCA
ASO-023	25	ACATCTCCAGACCATCTCTCACTAA
ASO-024	25	ATCTCCAGACCATCTCTCACTAAGA
ASO-025	18	CCAGACCAUCUCUCACUA
ASO-026	18	UCCAGACCAUCUCUCACU
ASO-027	18	CUCCAGACCAUCUCUCAC
ASO-028	18	UCUCCAGACCAUCUCUCA
ASO-029	18	AUCUCCAGACCAUCUCUC
ASO-030	18	CAUCUCCAGACCAUCUCU
ASO-031	18	ACAUCUCCAGACCAUCUC
ASO-032	18	GACAUCUCCAGACCAUCU
ASO-033	18	AGACAUCUCCAGACCAUC
ASO-034	18	CAGACAUCUCCAGACCAU
ASO-035	18	CCAGACAUCUCCAGACCA
ASO-036	18	UCCAGACAUCUCCAGACC
ASO-037	18	AUCCAGACAUCUCCAGAC
ASO-038	18	CAUCCAGACAUCUCCAGA
ASO-039	18	GCAUCCAGACAUCUCCAG
ASO-040	18	AGCAUCCAGACAUCUCCA
ASO-041	18	GAGCAUCCAGACAUCUCC
ASO-042	18	UGAGCAUCCAGACAUCUC
ASO-043	18	CUGAGCAUCCAGACAUCU
ASO-044	18	UCUGAGCAUCCAGACAUC
ASO-045	18	CUCUGAGCAUCCAGACAU
ASO-046	18	GCUCUGAGCAUCCAGACA
ASO-047	18	CGCUCUGAGCAUCCAGAC
ASO-048	21	UCUCCAGACCAUCUCUCACUA
ASO-049	21	AUCUCCAGACCAUCUCUCACU
ASO-050	21	CAUCUCCAGACCAUCUCUCAC
ASO-051	21	ACAUCUCCAGACCAUCUCUCA
ASO-052	21	GACAUCUCCAGACCAUCUCUC
ASO-053	21	CAGACAUCUCCAGACCAUCUC
ASO-054	21	CCAGACAUCUCCAGACCAUCU
ASO-055	21	UCCAGACAUCUCCAGACCAUC
ASO-056	21	AUCCAGACAUCUCCAGACCAU
ASO-057	21	CAUCCAGACAUCUCCAGACCA
ASO-058	21	AGCAUCCAGACAUCUCCAGAC
ASO-059	21	GAGCAUCCAGACAUCUCCAGA
ASO-060	21	UGAGCAUCCAGACAUCUCCAG
ASO-061	21	CUGAGCAUCCAGACAUCUCCA
ASO-062	21	UCUGAGCAUCCAGACAUCUCC
ASO-063	21	CUCUGAGCAUCCAGACAUCUC
ASO-064	21	GCUCUGAGCAUCCAGACAUCU
ASO-065	21	CGCUCUGAGCAUCCAGACAUC
ASO-066	19	CAUCCAGACAUCUCCAGAC
ASO-067	19	AUCCAGACAUCUCCAGACC
ASO-004-01	23	CAGACATCTCCAGACCATCTCTC
ASO-004-02	21	AGACATCTCCAGACCATCTCT
ASO-004-03	19	GACATCTCCAGACCATCTC
ASO-004-04	17	ACATCTCCAGACCATCT
ASO-005-01	23	AGCATCCAGACATCTCCAGACCA
ASO-005-02	21	GCATCCAGACATCTCCAGACC
ASO-005-03	19	CATCCAGACATCTCCAGAC
ASO-005-04	17	ATCCAGACATCTCCAGA

Supplementary Figure 2: List of ASO sequences examined in the micro-tiling and optimization of ASO length phase. All ASO sequences initially were synthesized using 2'-O-Methyl base chemistry and phosphorothioate backbone.

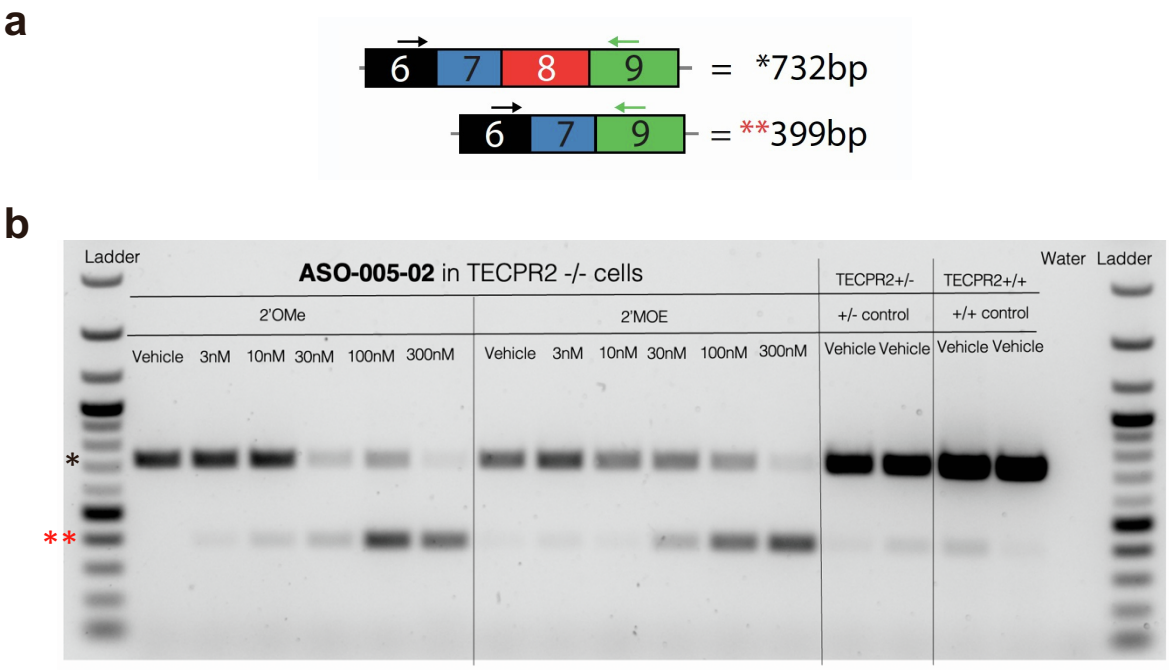

Supplementary Figure 3: Comparison of *TECPR2* Exon 8 skipping activity in TECPR2-/- patient-derived fibroblasts induced by ASO-005-02 sequence synthesized with 2'-O-Methyl (2'OMe) versus 2'-MOE RNA base chemistry. a, Diagram of RT-PCR assay and PCR amplicons to be obtained when *TECPR2* exon 8 is skipped in human fibroblast. **b**, DNA gel inverted image showing PCR results for fibroblast cells derived from *TECPR2-/-* patient treated for 5 days with ASO-005-02 sequence synthesized using two different types of ASO RNA base chemistry (2'-O-methyl (2'OMe) and 2'MOE) and 5 different concentrations (3 nM to 300 nM). Clear enrichment of lower PCR product (~399bp, highlighted by **) can be detected in fibroblast samples treated with either ASO chemistry at 30 nM to 300 nM compared to negative control conditions (vehicle).

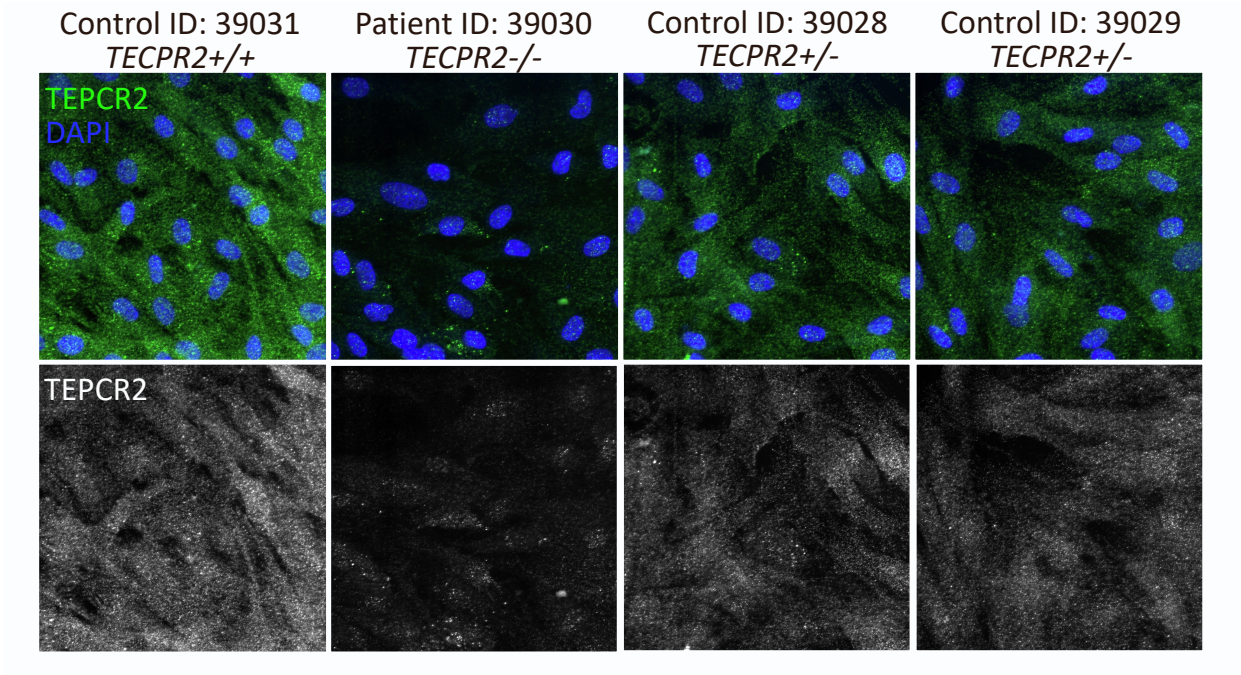

Supplementary Figure 4: Immunofluorescence staining for TECPR2 protein in fibroblast cell lines derived from SPG49 patient and healthy family members. Fibroblast cell lines were generated from skin punch biopsies obtained from the *TECPR2-/-* patient (Cell Line ID: 39030), from a *TECPR2+/+* family member (39031), and from two *TECPR2+/-* family members heterozygous for the *TECPR2* mutation (39028 and 39029). Cultured fibroblasts were analyzed by immunofluorescence staining for TECPR2 protein using a rabbit polyclonal antibody raised against human TECPR2 as the primary antibody. The top row shows the immunofluorescence signal for TECPR2 (green) and nuclear DAPI staining (blue). The bottom row shows the immunofluorescence signal for TECPR2 only. The first column shows immunocytochemistry analysis of homozygous wild type *TECPR2+/+*. The second column shows analysis of *TECPR2-/-* SPG49 patient fibroblasts. The third and fourth columns show analysis of heterozygous *TECPR2+/-* fibroblast cell lines from two of the patient's family members that are heterozygous for the patient's *TECPR2* mutation. As seen in column two, there is a substantial loss of TECPR2 immunoreactivity signal in fibroblast cells derived from the SPG49 patient, compared to either *TECPR2+/+* cells or *TECPR2+/-* cells.

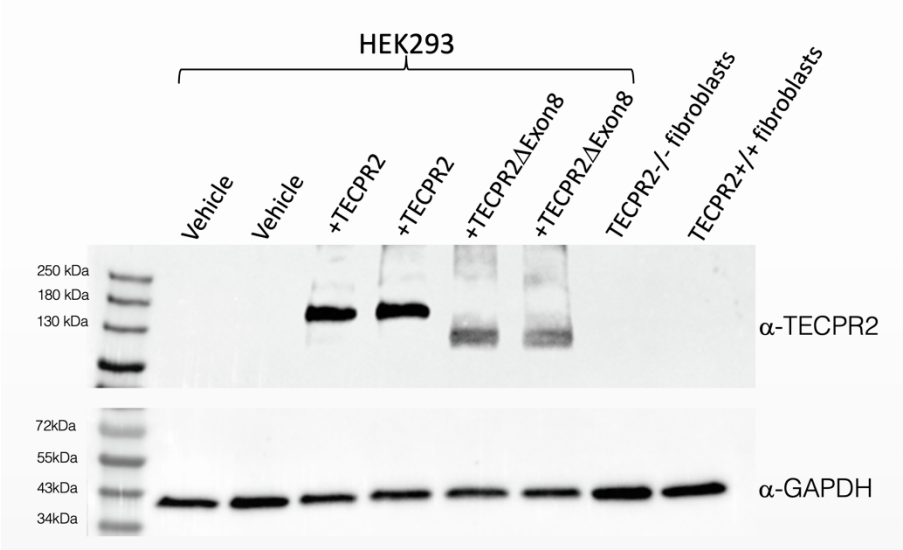

Supplementary Figure 5: TECPR2 antibody can detect overexpression of TECPR2 full length protein and TECPR2ΔExon8 protein variants, but not endogenous levels of TECPR2 protein in HEK293 cells and human fibroblasts. To determine if the TECPR2 polyclonal antibody used for immunocytochemistry assays could detect TECPR2 full length and TECPR2ΔExon8 protein levels, DNA expression constructs containing either cDNA variant were transfected into HEK293 cells using Lipofectamine. Protein lysates were collected after 72 hours from each of 2 replicate wells per condition and separated by SDS-PAGE after loading 30 µg of total HEK293 protein lysate. Immunoblotting assays with the TECPR2 polyclonal antibody detected a protein band at ~180KDa, corresponding to the predicted size of full length TECPR2 in samples treated with the TECPR2 cDNA expression construct, and a lower molecular weight species corresponding to a shorter variant of TECPR2 lacking 111 amino acids from *TECPR2* Exon 8 in samples transfected with the TECPR2ΔExon8 cDNA. Endogenous TECPR2 protein signal was not detected in either HEK293 cell extracts treated with vehicle or in 25 µg protein lysates obtained from TECPR2+/+ and TECPR2-/- fibroblasts. Immunoblotting against housekeeping protein GAPDH was used to demonstrate protein loading. These results suggest that using immunoblotting to measure endogenous levels of TECPR2 and TECPR2ΔExon8 protein variant induced by Exon 8 skipping in the human fibroblast assay is not feasible with this immunoreagent.

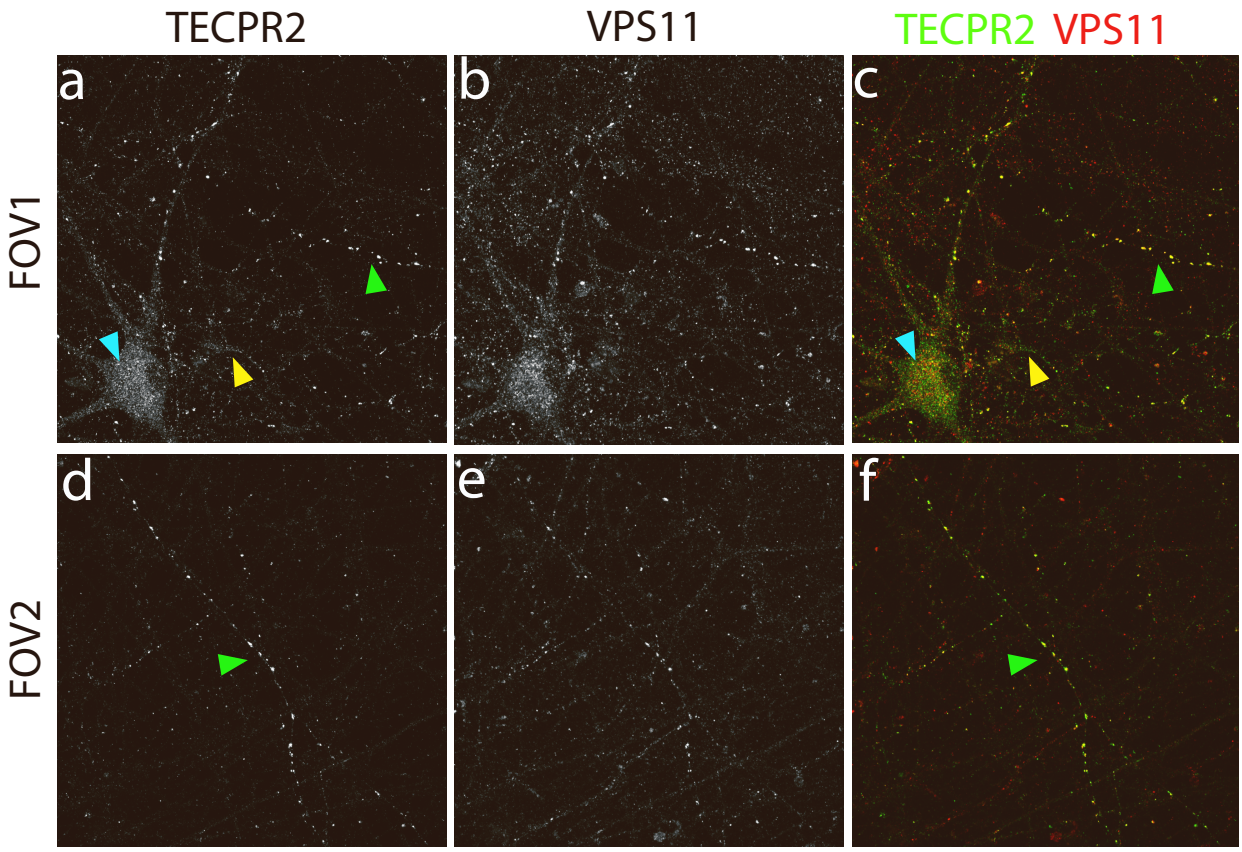

Supplementary Figure 6: Immunocytochemistry analyses showing co-localization of TECPR2 protein with vesicle-mediated trafficking protein VPS11 (Vacuolar Protein Sorting-associated protein 11 homolog) in *TECPR2*+/+ iPSC-derived neurons (DIV45). Two different fields of view (FOV1 and FOV2) are presented, with panels **a** and **d** showing TECPR2 immunoreactivity signal. In these panels, cyan arrowhead shows TECPR2 puncta localization in soma, yellow arrowhead shows small discrete TECPR2 positive puncta in neurites, and green arrowheads show rare large TECPR2 puncta in neuronal processes. Panels **b** and **e** show VPS11 immunoreactivity signal for the same FOV1 and FOV2, respectively. Significant overlap of TECPR2 (in green) and VPS11 (in red) immunoreactivity signal can be detected in the merged panels **c** and **f**, where the three arrowheads indicate the three different types of TECPR2/VPS11 positive puncta which can be detected by a yellow signal.

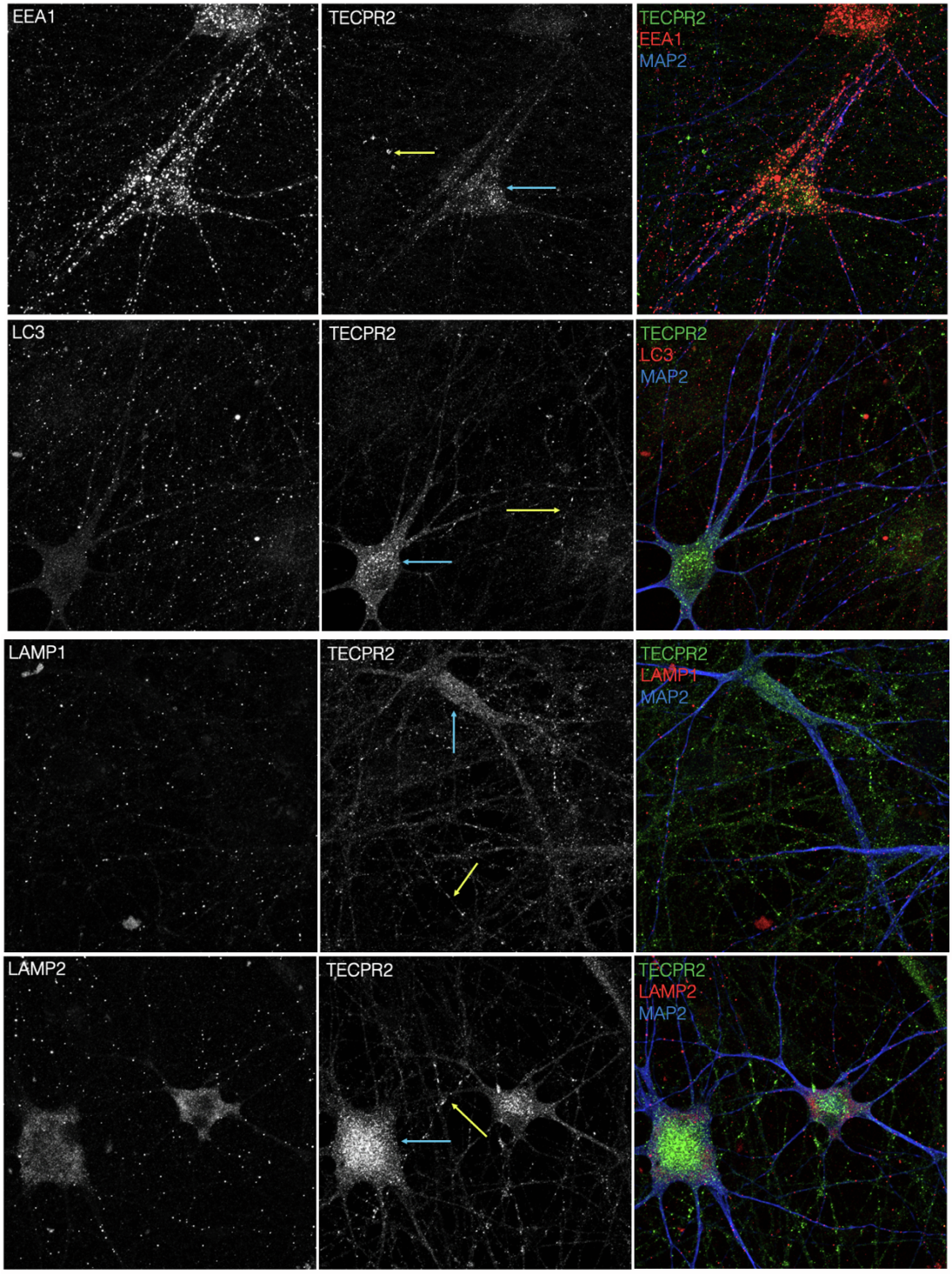

Supplementary Figure 7: Immunocytochemistry analyses showing lack of co-localization of TECPR2 protein puncta with additional autophagy and lysosomal markers in human iPSC-derived neurons. Given the reported association of TECPR2 with autophagy and ER export[1,4], we assessed co-localization of TECPR2 with EEA1 (Early Endosome Antigen 1), LAMP1 (Lysosomal-Associated Membrane Protein 1), LAMP2, and the autophagy cargo marker LC3 (Microtubule-Associated Protein 1A/1B-Light Chain 3) in *TECPR2*+/+ iPSC-derived NGN2 neurons (DIV45). We did not detect significant co-localization of TECPR2 with any of these markers, including in the large TECPR2-positive puncta as indicated by arrows in the panels above, suggesting that in these neurons, TECPR2 protein has a subcellular localization that is distinct from canonical endosomal, lysosomal and autophagosomal compartments.

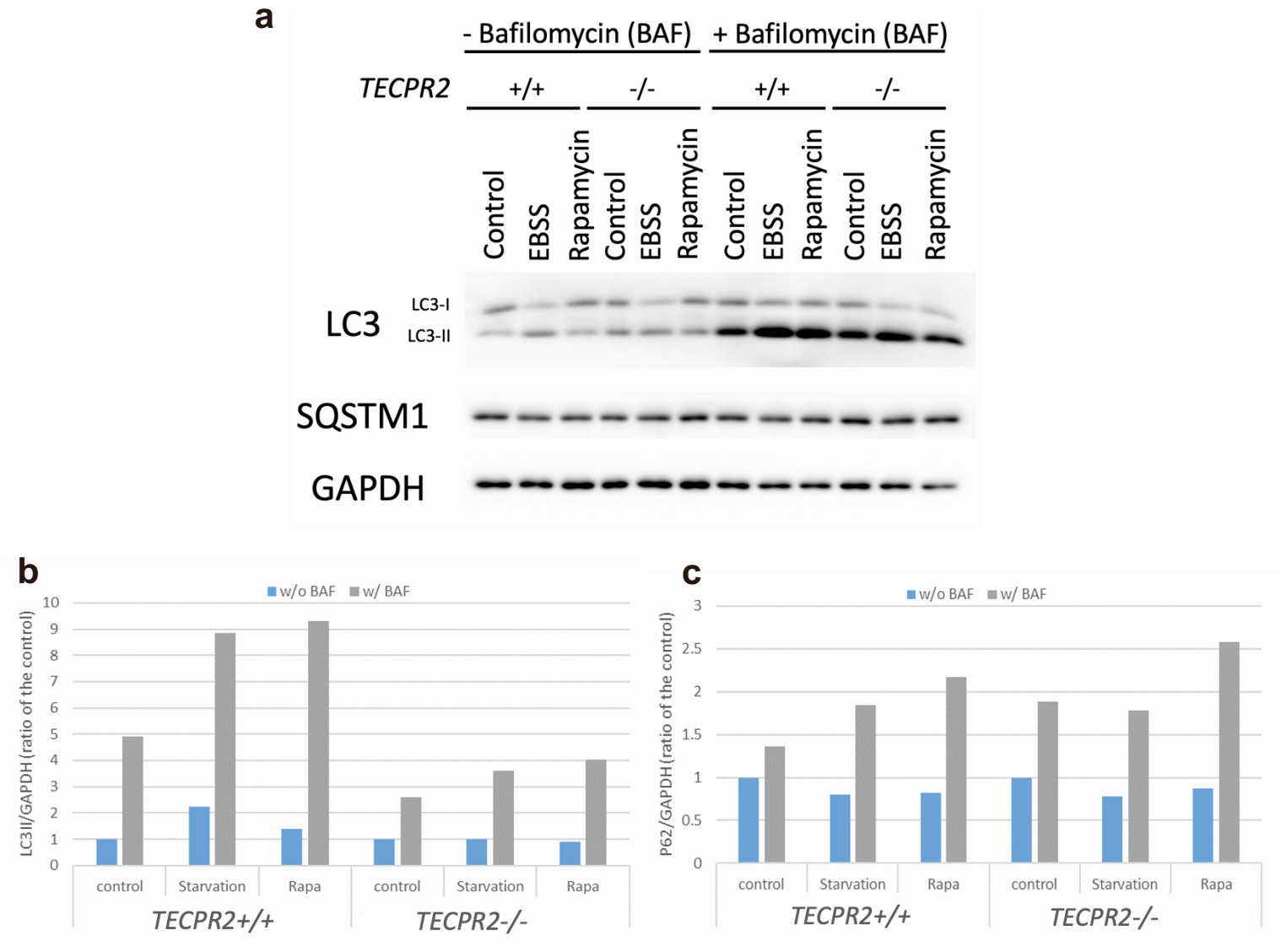

Supplementary Figure 8: Preliminary autophagy assays with *TECPR2-/-* patient and healthy *TECPR2+/+* control fibroblasts did not reveal a clear impact of loss of TECPR2 on basal autophagy or the response to autophagy inducers. a, MAP1LC3B (LC3) lipidation and SQSTM1 (p62) protein levels in human *TECPR2+/+* and *TECPR2-/-* fibroblasts cultured in complete medium (control), starvation inducing medium (EBSS), or complete medium supplemented with 5 uM Rapamycin (RAPA), with or without 25 nM Bafilomycin A1 (BAF) treatment for 6 hours. Levels for the housekeeping protein GAPDH were used as a loading control. **b**, Lipidated LC3 (LC3-II) and **c**, SQSTM1 (p62) protein levels normalized to GAPDH were compared to control condition for each *TECPR2* genotype. While *TECPR2-/-* cells appear to exhibit a mild defect in LC3-II lipidation in response to conventional autophagy activators (starvation and Rapamycin administration) as compared to *TECPR2-/-* cells (which can be maximally appreciated in the presence of the lysosomal inhibitor bafilomycin A1), the lysosome-dependent degradation of autophagy substrates like p62 is not affected by loss of TECPR2. Given that these fibroblast cell lines are not syngeneic, additional studies using multiple cell lines and other cell types such as neurons are warranted.

a

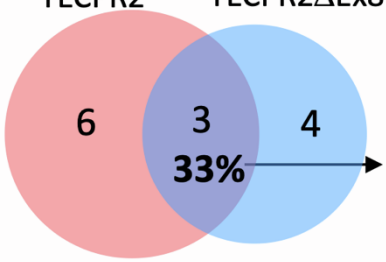

TECPR2 and TECPR2ΔEx8 interactions

Protein	TECPR2 logOdds	TECPR2ΔEx8 logOdds
FLNA	79.1	65.16
MCM3	45.24	56.81
PRKDC	49.62	72.64

	Protein	TECPR2 logOdds	TECPR2ΔEx8 logOdds
TECPR2 interactions	EPPK1	40.2	25.67
	USP7	71.75	38.5
	VPS16	42.89	
	VPS18	55.93	
	VPS33A	58.81	
	VPS41	51.59	
TECPR2ΔEx8 interactions	DNAJA1	26.68	45.76
	MCM5	31.13	44.31
	MCM7	29.13	43.79
	USP9X	39.94	42.85

b

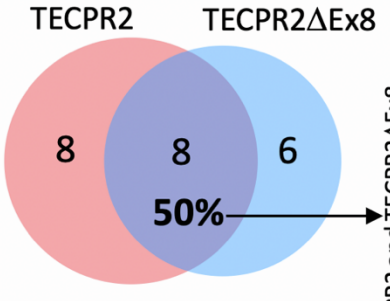

TECPR2 and TECPR2ΔEx8 interactions

Protein	TECPR2 logOdds	TECPR2ΔEx8 logOdds
FLNA	79.1	65.16
HSPH1	32.6	32.6
MCM3	45.24	56.81
MCM5	31.13	44.31
PFKP	37.04	35.57
PRKDC	49.62	72.64
USP7	71.75	38.5
USP9X	39.94	42.85

	Protein	TECPR2 logOdds	TECPR2ΔEx8 logOdds
TECPR2 interactions	VPS16	42.89	
	VPS18	55.93	
	VPS33A	58.81	
	VPS41	51.59	
	EPPK1	40.2	25.67
	IRS2	34.08	25.18
	NUP155	35.06	23.19
	PARD3	32.64	26.69
TECPR2ΔEx8 interactions	ACLY	25.18	34.08
	BLOC1S5	26.71	34.1
	DNAJA1	26.68	45.76
	DNAJA2	20.69	32.62
	MCM7	29.13	43.79
	SERPINH1	17.63	32.62

c

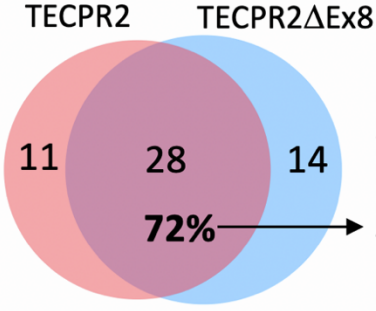

TECPR2 and TECPR2ΔEx8 interactions

Protein	TECPR2 logOdds	TECPR2ΔEx8 logOdds
ACLY	25.18	34.08
ACOT9	20.69	29.67
BLOC1S5	26.71	34.1
CCT2	23.5	22.31
CYTIP	26.71	26.69
DNAJA1	26.68	45.76
DNAJA2	20.69	32.62
DNAJC7	23.71	25.2
DOCK6	20.69	20.68
DOCK7	20.69	20.68
DTNBP1	23.71	29.67
EPPK1	40.2	25.67
FLNA	79.1	65.16
HSPA4L	23.68	20.66
HSPH1	32.6	32.6
IRS2	34.08	25.18
MCM3	45.24	56.81
MCM5	31.13	44.31
MCM7	29.13	43.79
MTHFD1L	28.2	20.68
NUP155	35.06	23.19
PARD3	32.64	26.69
PFKP	37.04	35.57
PRKDC	49.62	72.64
SNX27	26.71	26.69
UBA1	28.16	29.65
USP7	71.75	38.5
USP9X	39.94	42.85

	Protein	TECPR2 logOdds	TECPR2ΔEx8 logOdds
TECPR2 interactions	BLOC1S3	25.21	19.16
	CSNK2A1	28.2	
	CSNK2A2	26.71	
	CSNK2A3	28.2	
	DYNC1H1	25.21	19.16
	KPNA1	23.21	
	PLK1	22.21	11.33
	VPS16	42.89	
	VPS18	55.93	
	VPS33A	58.81	
	VPS41	51.59	
TECPR2ΔEx8 interactions	CARNS1	19.17	22.19
	CCT3	15.3	24.44
	CCT5	13.63	21.14
	GMPS	14.53	20.68
	HUWE1	19.17	22.19
	NUDC	17.63	20.68
	PGAM5	18.84	24.28
	PLS1	19.14	23.68
	PLS3	19.14	23.68
	PSMD2	9.7	25.2
	RUVBL1	12.91	22.17
	SERPINH1	17.63	32.62
	SLC25A1	14.53	20.68
	USP11	17.63	25.2

Supplementary Figure 9: Preliminary interactome studies in HEK293 cells with stable expression of HA-tagged TECPR2 and TECPR2ΔExon8 protein variants suggest that a significant percentage (33%-72%) of protein interactors with full-length TECPR2 also interact with TECPR2ΔEx8. To identify potential TECPR2 protein interactors, and to compare interactors of full-length TECPR2 and TECPR2ΔEx8 in cells, pull-down experiments using stable expression of HA-tagged TECPR2 (full-length) and HA-tagged TECPR2ΔEx8 in *TECPR2-/-* HEK293 cells were performed, followed by identification of proteins that were pulled down using mass spectrometry-based proteomics. A stringent Bayesian False Discovery Rate (BFDR) of 0.01 statistical threshold was used to define interactors. Log of Odds ratios (LOR) of 40, 30 and 20 were applied to the identified interactors to define likely significant interaction candidates over a range of statistical thresholds (see methods for additional experimental details). **a-c**, Venn diagrams highlighting the percentage of TECPR2 protein interactions that are retained by the TECPR2ΔEx8 variant, along with tables listing the candidate protein interactors defined using different Log of Odds ratios (LOR) statistical thresholds: (**a**) LOR 40, with 3 out of 9 (33%) defined candidate interactions for TECPR2 retained by TECPR2ΔEx8, (**b**) LOR 30, with 8 out 16 (50%) defined candidate interactions for TECPR2 retained by TECPR2ΔEx8, (**c**) LOR 20, with 28 out 39 (72%) defined candidate interactions TECPR2 retained by TECPR2ΔEx8. From these analyses, there is evidence that a significant percent of interactors with full-length TECPR2 also interact with TECPR2ΔEx8. The estimated percentage of retained interactions ranges from 33% - 72%, depending on the statistical thresholds used for the analysis. It is not straightforward to describe potential TECPR2 functions that may be retained by TECPR2ΔEx8 or to estimate how this may relate to therapeutic efficacy of ASO-005-02 from examining the set of retained protein interactors. It is also of note that there are 8 proteins (VPS41, VPS33A, VPS16, VPS18, CSKN2A1, CSKN2A2, CSKN2A3 and KPNA1) that were identified as interactors of TECPR2, yet not found to interact with TECPR2ΔEx8. TECPR2 functions associated with interactions with these proteins, although unknown, may not be restored by TECPR2ΔEx8. There was not strong evidence that any proteins interact exclusively with the TECPR2ΔEx8 form. However, a few proteins seem to have a stronger interaction with TECPR2ΔEx8 than the full-length form: DNAJA1, DNAJA2, MCM3, MCM5 and MCM7. One of the challenges of this approach is that it is not possible to predict which TECPR2 interactome mediated functions may be retained by TECPR2ΔEx8 or to estimate how this may relate to therapeutic efficacy of ASO-005-02. This is in large part due to the state of limited knowledge regarding the function of TECPR2 and the functions of its interacting partners.

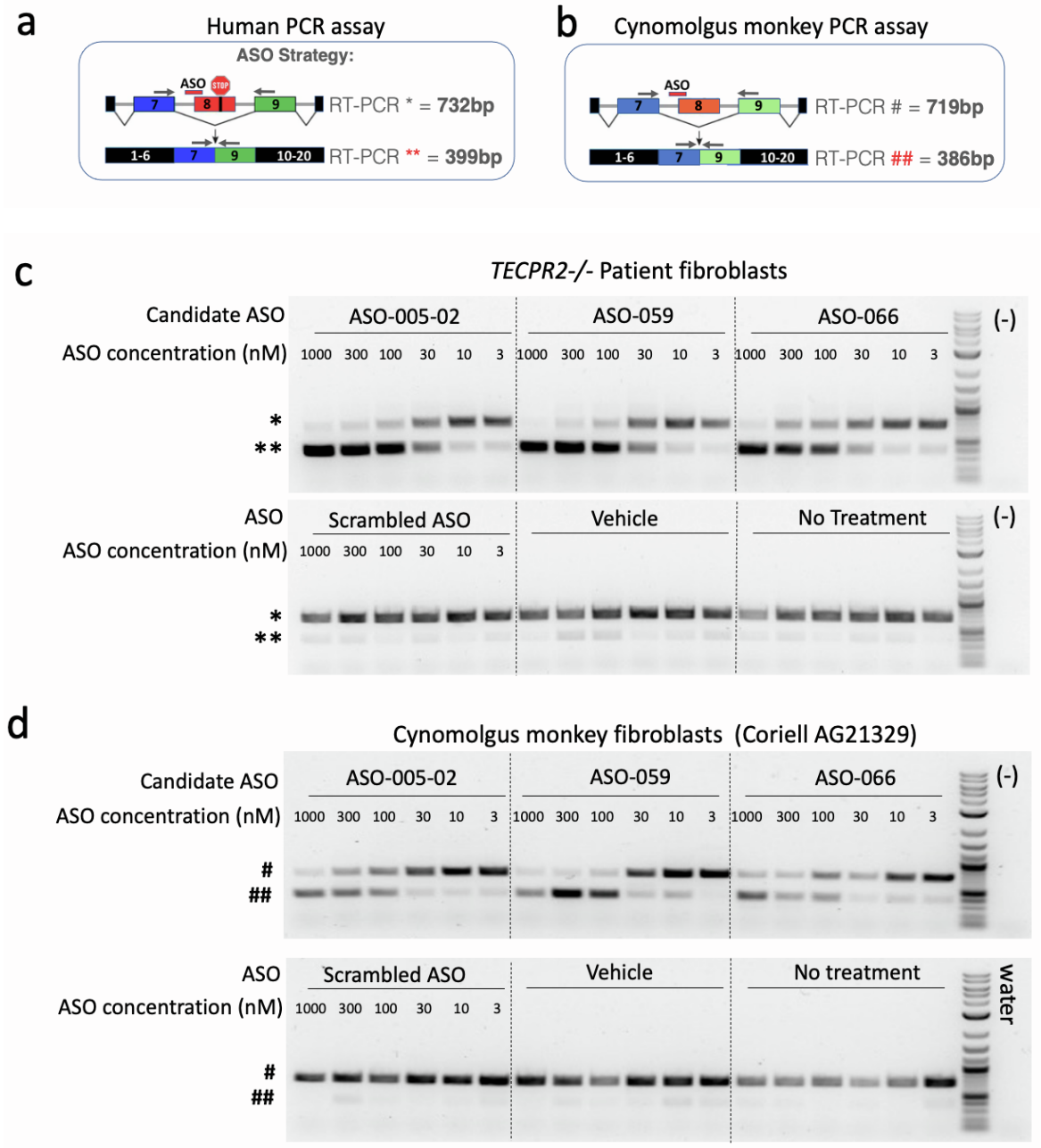

Supplementary Figure 10: Assessment of top 3 ASO lead candidates in cultured cynomolgus monkey fibroblasts prior to *in vivo* tolerability studies. a,b Diagram of RT-PCR assay and PCR amplicons to be obtained when *TECPR2* exon 8 is skipped in patient-derived cells (a) or in cultured cynomolgus monkey fibroblasts (b). **c**, DNA gel inverted images showing PCR results for patient fibroblasts treated with ASO leads ASO-005-02, ASO-059 and ASO-066 at different concentrations (1000 nM to 3 nM). Enrichment of lower PCR product (~399bp, highlighted by **) can be detected in samples treated with 30 nM to 1000 nM of each of the 3 ASOs compared to negative control conditions (scrambled non-targeting ASO sequence, vehicle, and No Treatment). **d**, DNA gel inverted images showing PCR results for cultured cynomolgus fibroblasts treated with ASO leads ASO-005-02, ASO-059 and ASO-066 at different concentrations (1000 nM to 3 nM). Enrichment of lower PCR product (~386bp, highlighted by ##) can be detected in samples treated with 100 nM to 1000 nM of each of the 3 ASOs compared to negative control conditions (scrambled non-targeting ASO sequence, vehicle, and No Treatment).

The objective of this NHP study was to determine the tolerability and lead selection of 3 candidate antisense oligonucleotides (ASOs): ASO-059 (Lot ID: QS0321489-05), ASO-005-02 (QS0321490-05), ASO-066 (QS0321491-05) when given by a single intrathecal injection to monkeys. In addition, the biodistribution characteristics of each candidate were determined. The study design was as follows:

Group No.	Test Material	Dose Level (mg/dose)	Dose Volume (mL/dose)	Dose Concentration (mg/mL)	Animal Numbers	
					Main Study	
					Males	Females
1	Reference Item (Elliotts B)	0	1	0	1001	-
2	QS0321489-05 (ASO-059)	20	1	20	2001	2501
3	QS0321490-05 (ASO-005-02)	20	1	20	3001	3501
4	QS0321491-05 (ASO-066)	20	1	20	4001	4501

QS0321489-05, QS0321490-05, and QS0321491-05, formulated in Elliotts B solution, was administered by direct intrathecal puncture at the lumbar level on Day 1. The following parameters and end points were evaluated in this study: mortality, clinical observations, body weights, neurological examinations, cerebrospinal fluid (CSF) and tissue bioanalysis (samples collected at necropsy), tissue mRNA splicing analysis, gross necropsy findings, and histopathological examinations.

There was no mortality during the study.

There were no QS0321489-05-, QS0321490-05-, and QS0321491-05-related effects on body weights and pathology findings (macroscopic and microscopic).

Administration of QS0321489-05, QS0321490-05, and QS0321491-05 resulted in similar clinical signs, consisting of tremors, decreased activity, partly closed eyes, hunched posture, and/or emesis. These clinical observations were generally more prominent in females; however due to the small population size in the study, this should be interpreted with caution. Clinical signs were noted as early as 4 hours post-dose on Day 1 and had generally resolved by the following day. These clinical signs were consistent with findings in the animals' general attitude and motor function noted at the 5-hour post-dose neurological examination. Additionally, decreased muscle tone and/or flexor reflex were observed in one or both hindlimbs in Animal Nos. 2501, 3001, 3501, and 4501. Neurological changes were more prominent in Animal No. 3501 administered QS0321490-05 at 20 mg, which also demonstrated a lack of visual and tactile placing reactions of both hindlimbs. At 24 hours post-dose, decreased visual placing reactions and/or flexor reflexes (hindlimbs and forelimbs) were still evident but did not correlate with any abnormal clinical observations. There were no abnormal changes noted on Day 15.

Bioanalytical results for samples collected at necropsy showed that concentration of QS0321489-05 and QS0321491-05 in CSF was detected in 1 out of 2 animals (female only) and concentration of QS0321490-05 was detected in both animals. Concentration of QS0321489-05, QS0321490-05, or QS0321491-05 was detected in the tissue samples from both animals in each group. There was moderate inter-animal variability observed for all 3 ASOs and a trend towards QS0321490-05 generally yielding higher concentrations in many tissue samples.

Tissue mRNA splicing analysis demonstrated that there was clear evidence of *TECPR2* exon8-skipping activity in CNS tissue samples. A clear relationship between the degree of exon8 skipping and ASO concentration was observed among a subset of CNS tissues analyzed from the two animals treated with QS0321490-05.

In conclusion, administration of QS0321489-05, QS0321490-05, or QS0321491-05 by a single intrathecal injection resulted in transient clinical signs and neurological changes, which were similar in nature for all 3 ASOs. Concentrations of QS0321489-05, QS0321490-05, or QS0321491-05 were detected in all tissue samples and generally in 1 of 2 CSF samples. Tissue mRNA splicing analysis revealed that QS0321490-05 demonstrated the best exon8-skipping activity among the three ASOs; and therefore, was chosen as the lead candidate for the subsequent study.

Supplementary Figure 11: Summary report for non-human primate tolerability study.

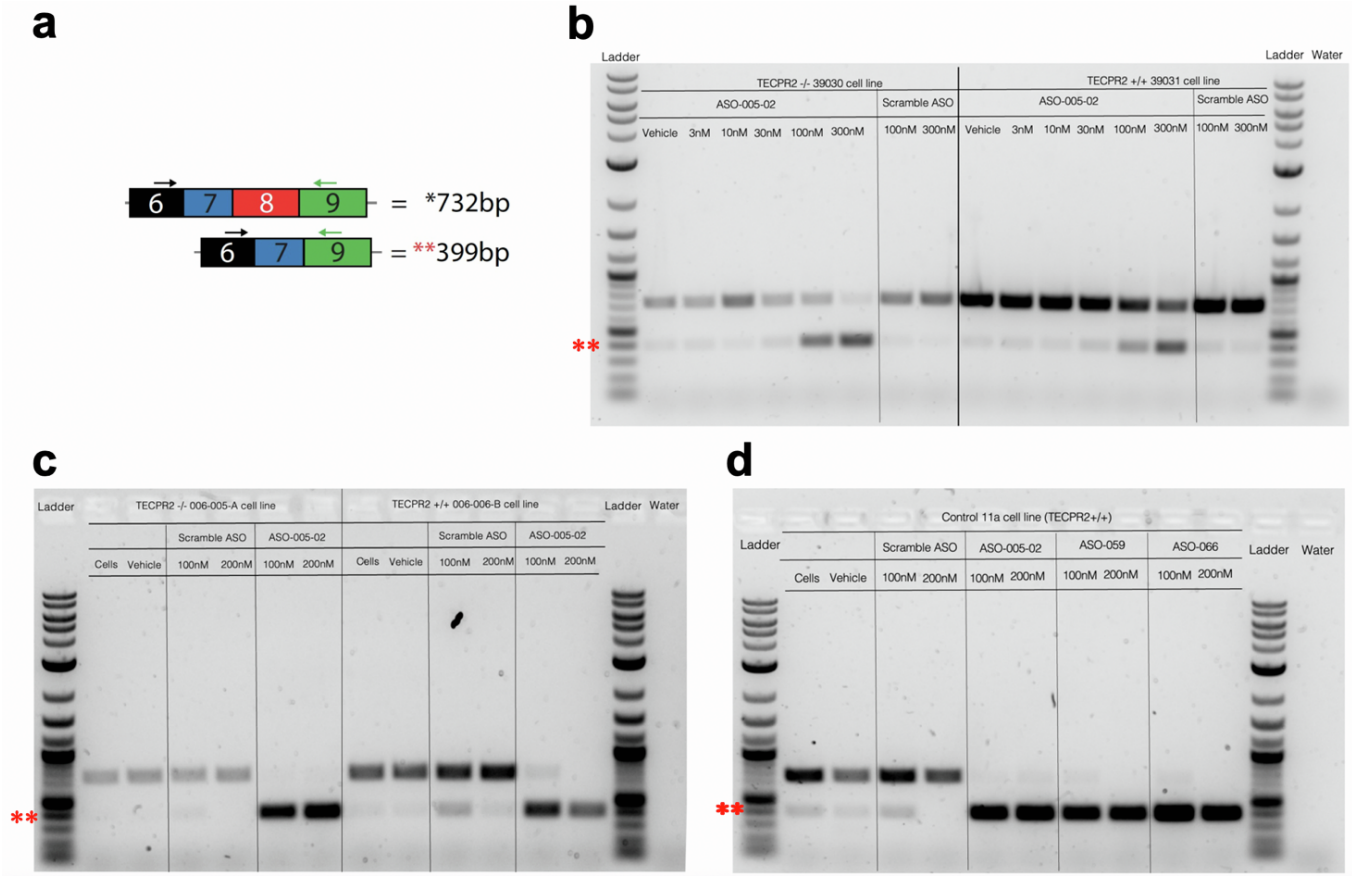

Supplementary Figure 12: Top ASO lead candidate (ASO-005-02) induces TECPR2 Exon 8 skipping activity in *TECPR2*+/+ control cellular reagents (dermal fibroblasts and human iPS cell-derived neurons). a, Diagram of RT-PCR assay and PCR amplicons to be obtained when *TECPR2* exon 8 is skipped in human fibroblast and iPS cell-derived neurons. **b**, DNA gel inverted image showing PCR results for fibroblast cells derived from *TECPR2-/-* patient (39030 cell line) and *TECPR2*+/+ healthy control (39031 cell line) treated for 5 days with ASO lead candidate ASO-005-02, at different concentrations (3 nM to 300 nM). Clear enrichment of lower PCR product (~399bp, highlighted by **) can be detected in samples treated with 100 nM to 300 nM compared to negative control conditions (scrambled non-targeting ASO sequence and vehicle). **c**, DNA gel inverted image showing PCR results for cultured human iPS cell-derived neurons derived from *TECPR2-/-* patient (006-005-A cell line) and *TECPR2*+/+ healthy control (006-006B cell line) treated for 7 days with ASO lead candidate ASO-005-02, at two different concentrations (100 nM and 200 nM). Clear enrichment of lower PCR product (~399bp, highlighted by **) can be detected at both concentrations compared to negative control conditions (scrambled non-targeting ASO sequence, vehicle and untreated cells). For this experiment, ASO was delivered into the cultured neurons using optimized transfection conditions with a polypeptide delivery reagent (vehicle). **d**, DNA gel inverted image showing PCR results for cultured human neurons derived from a *TECPR2*+/+ iPS cell line (Control 11a cell line) obtained from a different healthy donor. Cultured neurons were treated for 7 days with the top ASO lead candidate (ASO-005-02) and two back-up candidates (ASO-059 and ASO-066) at two different concentrations (100 nM and 200 nM). Clear enrichment of lower PCR product (~399bp, highlighted by **) can be detected at both concentrations compared to negative control conditions (scrambled non-targeting ASO sequence, vehicle and untreated cells). For this experiment, ASO leads were delivered into the cultured neurons using optimized transfection conditions with a polypeptide delivery reagent (vehicle). "Water" for all PCR experiments indicates a negative control sample in which cDNA was not added to the PCR assay.

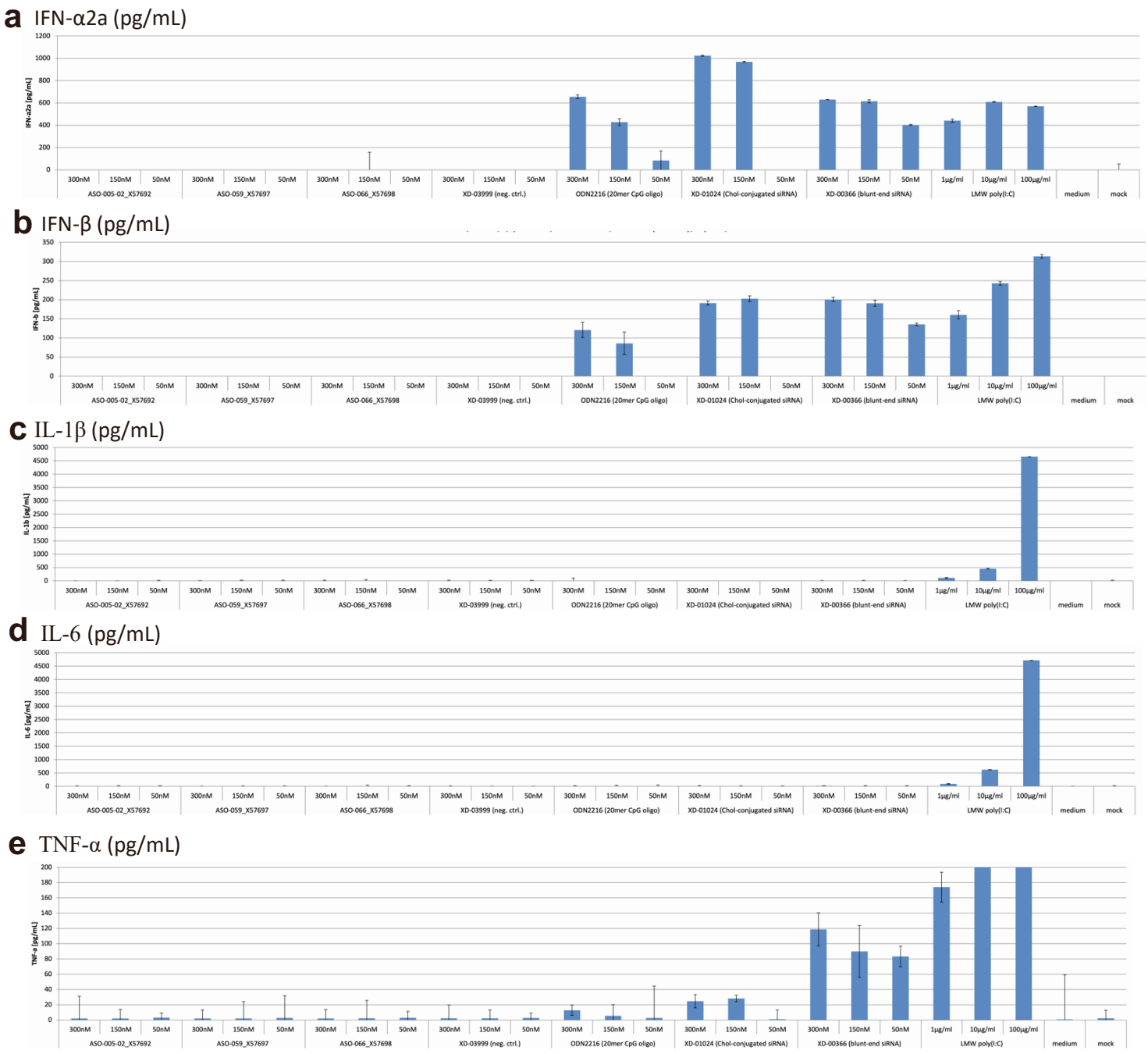

Supplementary Figure 13: ASO lead candidate (ASO-005-02) and two back-up candidates (ASO-059 and ASO-066) are inactive in human PBMC cytokine release assays. ASO molecules were delivered at 3 different concentrations (50 nM, 150 nM, 300 nM) into human peripheral blood mononuclear cells via lipid-based transfection (Lipofectamine 2000) and the levels for 5 different cytokines: (a) IFN-α2a, (b) IFN-β, (c) IL-1β, (d) IL-6, (e) TNF-α were measured and analyzed using MSD platform 24 hrs after transfection. None of the 3 ASO molecules tested induced upregulation in cytokine release. Multiple positive controls (inflammatory stimuli) were used, including a TLR7/8 agonist (XD-01024, a cholesterol-conjugated ApoB siRNA), a TLR9 agonist (ODN2216, a 20mer CpG oligo containing unmethylated CpG), a TLR7/8 agonist (XD-00366, a 25mer double-stranded, unmodified, blunt-ended LacZ RNA duplex), and a TLR3, RIG-I/MDA5 and PKR agonist (LMW poly(I:C): low molecular weight polyinosinic-polycytidylic acid). A chemically modified siRNA (XD-03999) against FVII was used as negative control.